JOURNAL OF MATERIALS SCIENCE 29 (1994) 2725–2733

EXAFS and molecular modelling studies of $Rb_{1-x}Bi_xF_{1+2x}$

P. A. COX
Department of Chemistry, University of Portsmouth, St Michael's Building, White Swan Road, Portsmouth, PO1 2DT, UK

C. R. A. CATLOW
Royal Institution of Great Britain, 21 Albermarle Street, London, W1X 4BX, UK

A. V. CHADWICK
Department of Chemistry, University of Kent at Canterbury, Canterbury, Kent, CT2 7NH, UK

The fluorite structured mixed metal fluorides $Rb_{1-x}Bi_xF_{1+2x}$ ($0.5 \leq x \geq 0.75$) are exceptionally good F^- ion conductors, a property which is clearly related to the mixed nature of the cation sub-lattice. Extended X-ray absorption fine structure (EXAFS) has been used to study the local structure of the two types of cation in $Rb_{1-x}Bi_xF_{1+2x}$ as a function of x. The results reveal marked differences for the local environments of Rb^+ and Bi^{3+}. Considerable short-range order develops as x deviates from 0.5, and this can be correlated with the relative conductivities of these materials. Molecular dynamics (MD) has been used to yield complementary information on structural properties. Simulations were performed for a series of temperatures between 80 K and 750 K. Excellent agreement between EXAFS and MD is obtained. A non-collinear interstitialcy mechanism is proposed for anion diffusion, which is seen to be the basis for more complex concerted processes.

1. Introduction

The high conductivities of materials of the form $ABiF_4$ (where A = K, Rb, Tl), which all form a fluorite-structured phase, have been demonstrated in a number of studies [1, 2]. $RbBiF_4$, which is prepared by standard solid-state procedures [1], displays three distinct phases, for which the phase transition temperatures are as follows:

$$\alpha \underset{553\,K}{\rightleftharpoons} \beta \underset{668\,K}{\rightleftharpoons} \gamma \underset{713\,K}{\rightleftharpoons} \text{Liquid}$$

Quenching will produce a meta-stable γ-phase sample. This fluorite-structured phase exhibits superionic behaviour, with a F^- ion conductivity which is several orders of magnitude higher than that of corresponding fluorite-structured compounds of similar lattice parameter such as β–PbF_2. The fluorite structure, shown in Fig. 1a, can be visualized as a cubic array of anions with half the cube-centre sites occupied by cations, which in the present case comprise Rb and Bi ions whose distribution shows no long range order.

Two detailed studies of γ-$RbBiF_4$ via powder neutron diffraction experiments have shown that high degrees of disorder are present on the anion sublattice. Matar [2] analysed his data on the basis of a single type of interstitial site, the (0.5, 0.33, 0.33) position in the unit cell (see Fig. 1b). Fitting data using this model yielded an R-factor of 8.5%, with 25% of the normal cube-corner sites vacant. Jordan [3] investigated a wide range of different interstitial models. The best R-factor of 3.9 was obtained with a model incorporating two types of interstitial. This contained 20% of F^- on the (0.5, 0.33, 0.33) site, 10% on the (0.425, 0.425, 0.425) site and the remaining 70% on the normal (0.25, 0.25, 0.25) sites. All these models assume that the Rb and Bi ions are randomly distributed over the available cation sites.

Additional fluorine ions may be accommodated by $ABiF_4$ phases to form solid solutions of formula $Rb_{1-x}Bi_xF_{1+2x}$ ($0.5 \leq x \geq 0.6$). Whereas these solid solutions are crystallographically disordered, for $x = 0.75$, a fully ordered material, $RbBi_3F_{10}$ may be prepared. This is isostructural with KY_3F_{10} (Fig. 2) and crystallizes in the $Fm3m$ space group [4]. It is characterized by the alternation in all three directions of the cubo-octahedral and fluorite-type clusters. The two different cation types occupy two distinct sites within the structure. Bi has eight nearest neighbours in the form of an antiprism. Rb has 16 surrounding fluorines in two shells separated by around 0.04 nm. The radial distribution of ions surrounding each type is shown in Fig. 3. Note how the relaxation of Bi ions away from the fluorite cation sites leads to a much less symmetrical environment.

As x is increased, the conductivity of $Rb_{1-x}Bi_xF_{1+2x}$ decreases despite the addition of charge compensating F^- ions. The temperature dependence of the conductivities for $RbBiF_4$, $Rb_{1-x}Bi_xF_{1+2x}$ ($x = 0.6$) and $RbBi_3F_{10}$ are shown in Fig. 4. A neutron diffraction

0022–2461

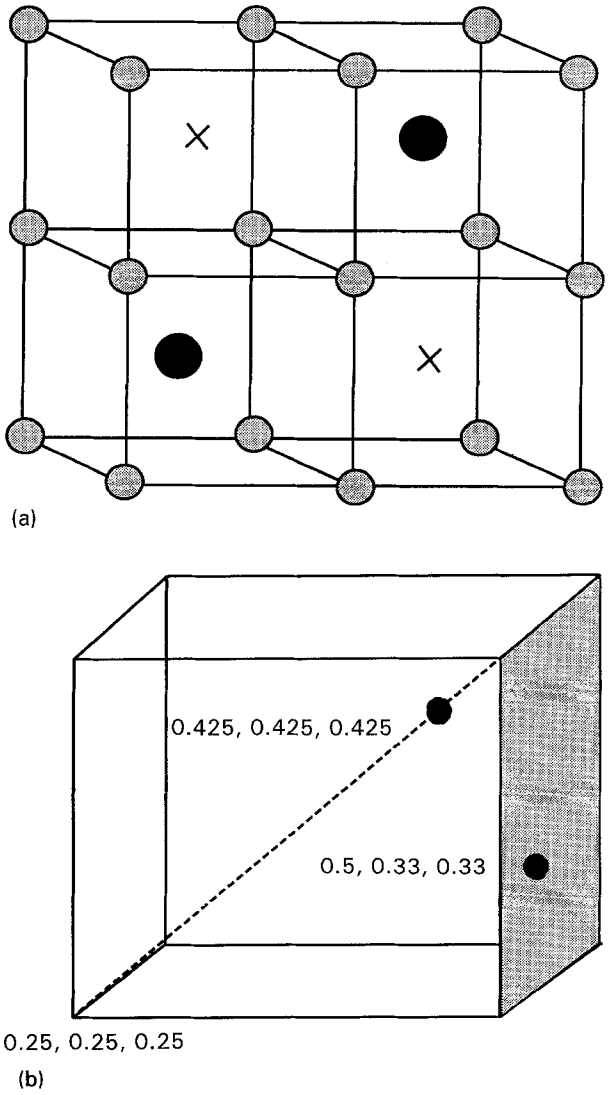

Figure 1 (a) The fluorite structure, and (b) the position of F^- interstitials in $RbBiF_4$ identified via neutron scattering. (⊚) anion, (×) interstitial, (●) cation.

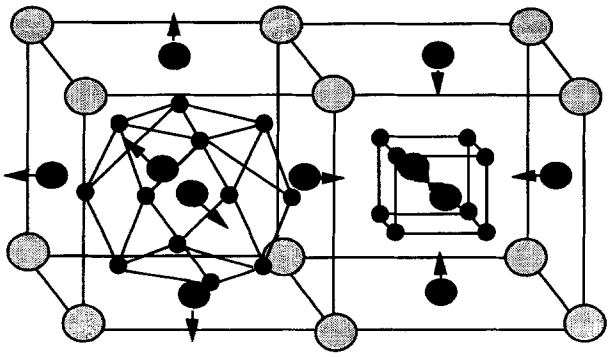

Figure 2 The $RbBi_3F_{10}$ structure. Note how the Bi^{3+} ions relax away from the face-centred sites. (•) F, (⊚) Rb, (●) Bi.

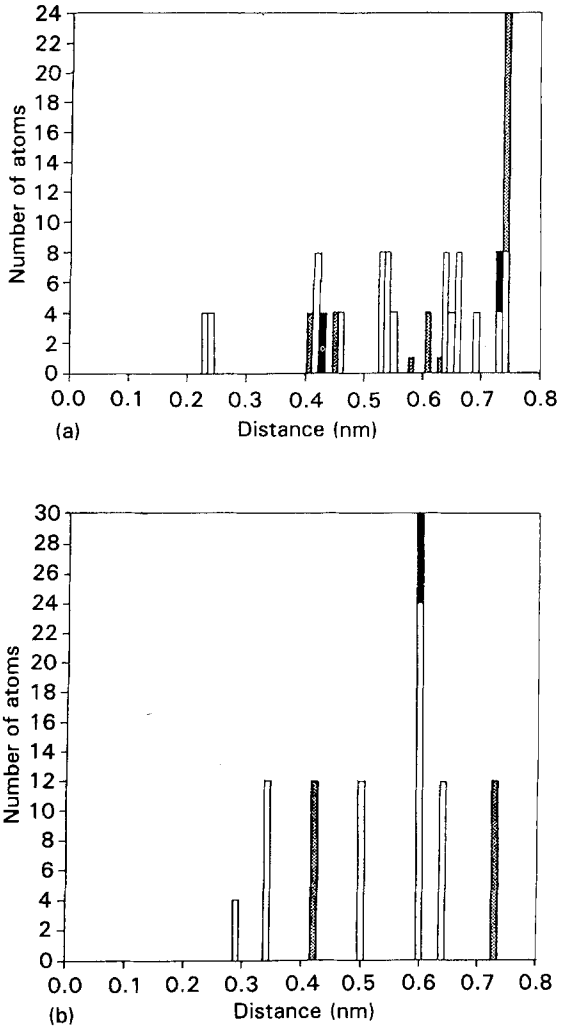

Figure 3 Radial distribution function for (a) Bi, and (b) Rb in $RbBi_3F_{10}$. (■) Rb, (▦) Bi, (□) F.

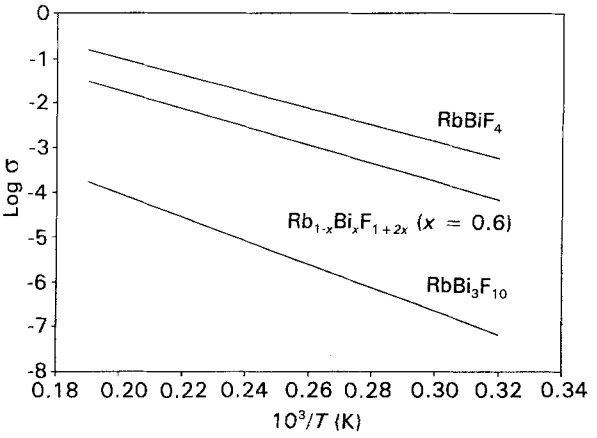

Figure 4 The temperature dependence of conductivities for $RbBiF_4$, $Rb_{1-x}Bi_xF_{1+2x}$ ($x = 0.6$) and $RbBi_3F_{10}$.

investigation found increasing numbers of fluorine ions at the (0.5, 0.33, 0.33) sites as x increases [1]. These positions are close to those of the 48*i* interstitial site occupied in the cubo-octahedron in $RbBi_3F_{10}$. Also a superstructure line is observed for $x > 0.5$ in the diffraction pattern. The authors suggested that this indicated the formation of precursor clusters in the solid solutions. These clusters "trap" additional F^- ions, and their contribution to the conductivity is lost.

In this work, we exploit two complementary techniques which are ideal for investigating the transport and structural properties in these materials. Extended X-ray absorption fine structure (EXAFS) yields unique information on local structural ordering within

condensed materials [5–7]. The EXAFS experiment measures the variation of a material's X-ray absorbance as a function of the incident X-ray energy at and beyond an absorption edge. Beyond the edge, oscillations are observed which arise from interference effects involving the photo-electron ejected from the absorbing atom and the fraction of the photoelectron backscattered by atoms surrounding the absorbing atom. Analysis of this oscillatory fine structure can reveal the local environment of specific atom types. Thus, it is generally useful in the study of disordered materials, and is particularly suitable in the present case as it enables us to investigate the local environment of Rb and Bi ions separately. In contrast, conventional diffraction techniques yield only limited information because data has been averaged over all unit cells in the structure. In analysing EXAFS data, it is useful to Fourier transform the normalized fine structure. This produces an approximate radial distribution function, in which features at low distances from the absorbing atom dominate the data.

Our second technique is that of molecular dynamics simulation. This method has been extensively applied to study the dynamical properties of condensed matter [8]. The techniques allow us to follow the time evolution of a system and yield a wealth of information including radial distribution functions, which in the present case can be usefully compared with EXAFS Fourier transforms. Diffusion coefficients may be calculated directly from the simulations and mechanisms of transport may also be deduced by plotting the coordinates of mobile particles.

2. EXAFS

2.1. Sample preparation

Samples of $RbBiF_4$, $Rb_{1-x}Bi_xF_{1+2x}$ ($x = 0.6$) and $RbBi_3F_{10}$ were prepared by mixing the parent fluorides in stoichiometric ratios and grinding to a fine powder. After pelleting, the mixture was heated at 400 °C for 12 h in a graphite crucible maintained under a dynamic vacuum. Samples were then held at a temperature just above the melting point for 1 h before being quenched in an ice-water bath.

2.2. Experimental details

Samples of each of the above were ground to a fine powder with a mortar and pestle, mixed with boron nitride and pressed into thin coherent pellets using a 13 mm die. The composition and thickness of two pellets for each sample were calculated, so as to yield an absorption ratio of 1.5 at the absorption edges of Rb and Bi. The samples were mounted in an evacuable furnace with Be windows and EXAFS data were obtained at 80 K. Spectra were also obtained for the model compounds RbF and Bi_2O_3 at room temperature in order to obtain phaseshifts for the unknowns. The X-ray source used was the Science and Engineering Research Council's Synchrotron Radiation Source (SRS) at Daresbury Laboratory, Cheshire. The SRS ran at 2 GeV with a typical beam current of 150 mA. A channel-cut Si(1 1 0) monochromator was used on station 7.1 of the SRS. Data reduction was performed using the EXAFS analysis suite which forms part of the SRS program library [9].

2.3. EXAFS results

2.3.1. $RbBiF_4$

Fig. 5 shows the k^2 weighted EXAFS and Fourier transform data obtained for the two cation edges at 80 K. Inspection of these shows that the local environment of each cation is highly disordered and that both types of cation have appreciably different short-range environments. Specifically,

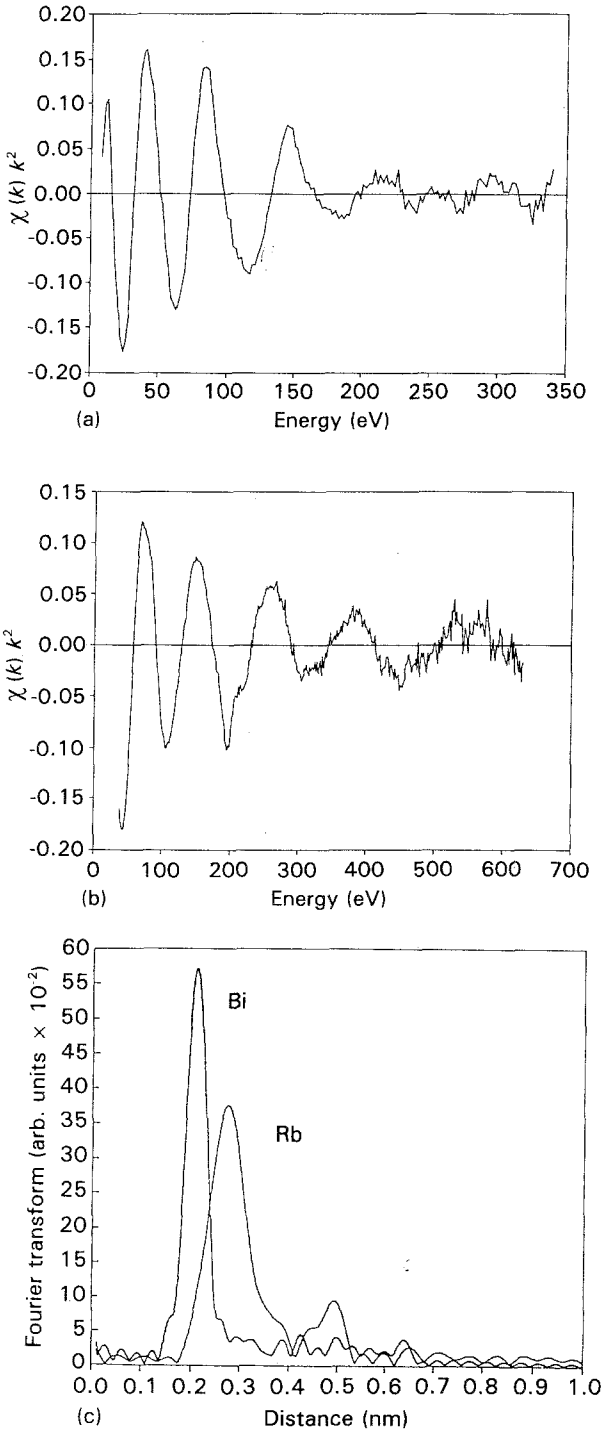

Figure 5 $RbBiF_4$: (a) Rb edge EXAFS; (b) Bi edge EXAFS; and (c) Bi edge and Rb edge Fourier transforms.

1. The two EXAFS spectra resemble one another in that each consists of a dominant frequency representing backscattering from the nearest neighbour shell only. This is confirmed by an examination of the Fourier transforms which consist of a single prevailing peak. In contrast, typical fluorite-structured materials such as CaF_2, show peaks in the Fourier transform to typically 0.6 or 0.7 nm [10]. We may conclude that the displacements of the atoms from their perfect lattice sites within $RbBiF_4$ is so great that backscattering from neighbours more distant that the first shell is diminished to the point where their EXAFS contributions are reduced to the noise level.

2. The peak in the Bi edge Fourier transform appears at around 0.06 nm less than for the Rb edge data, indicating a 0.06 nm difference between the Rb–F and Bi–F bond lengths.

The above suggest that the Bi ions "dictate" the structure by drawing F^- ions to form a tight coordination shell at a short distance. This leaves the Rb–F shell comparatively disordered.

2.3.2. $RbBi_3F_{10}$

The EXAFS spectra for the Rb and Bi edges of $RbBi_3F_{10}$ at 80 K are presented in Fig. 6. The spectra obtained display a marked contrast with those obtained for $RbBiF_4$, notably,

1. Both show a complex beating indicative of the superposition of sine waves with different component frequencies. It is clear that shells beyond the first nearest neighbours are contributing to the resultant spectra, and we can infer that short-range ordering in $RbBi_3F_{10}$ is significantly greater than in $RbBiF_4$. Further evidence for this point can be seen from the Fourier transforms which both contain more peaks than those obtained for $RbBiF_4$, indicating coherent backscattering from more distant shells. For the Rb edge, several peaks are observed out to 0.75 nm, a feature indicative of long-range ordering.

2. Fewer peaks are observed in the Bi edge than in the Rb edge Fourier transform. This may be attributed to the fact that Bi^{3+} ions are displaced from their centrosymmetric sites, resulting in a large spread of Bi neighbour distances in the Fourier transform beyond 0.6 nm. The Rb^+ ions, on the other hand, remain close to their centrosymmetric sites, which leads to additional structure in the Fourier transform and a more complex EXAFS spectrum.

A comparison with the radial distribution functions shown in Fig. 3 shows that the results are consistent with the proposed cubo-octahedral cluster structure for this material. Both F^- ion first peaks in the Fourier transforms show a reduced amplitude when compared with those obtained for $RbBiF_4$. Assuming that the phase shifts for $RbBiF_4$ and $RbBi_3F_{10}$ are the same, an increase in the static component of the Debye–Waller factor must be responsible for the observed reduction in amplitude obtained for $RbBi_3F_{10}$. This implies that Rb–F and Bi–F first neighbour

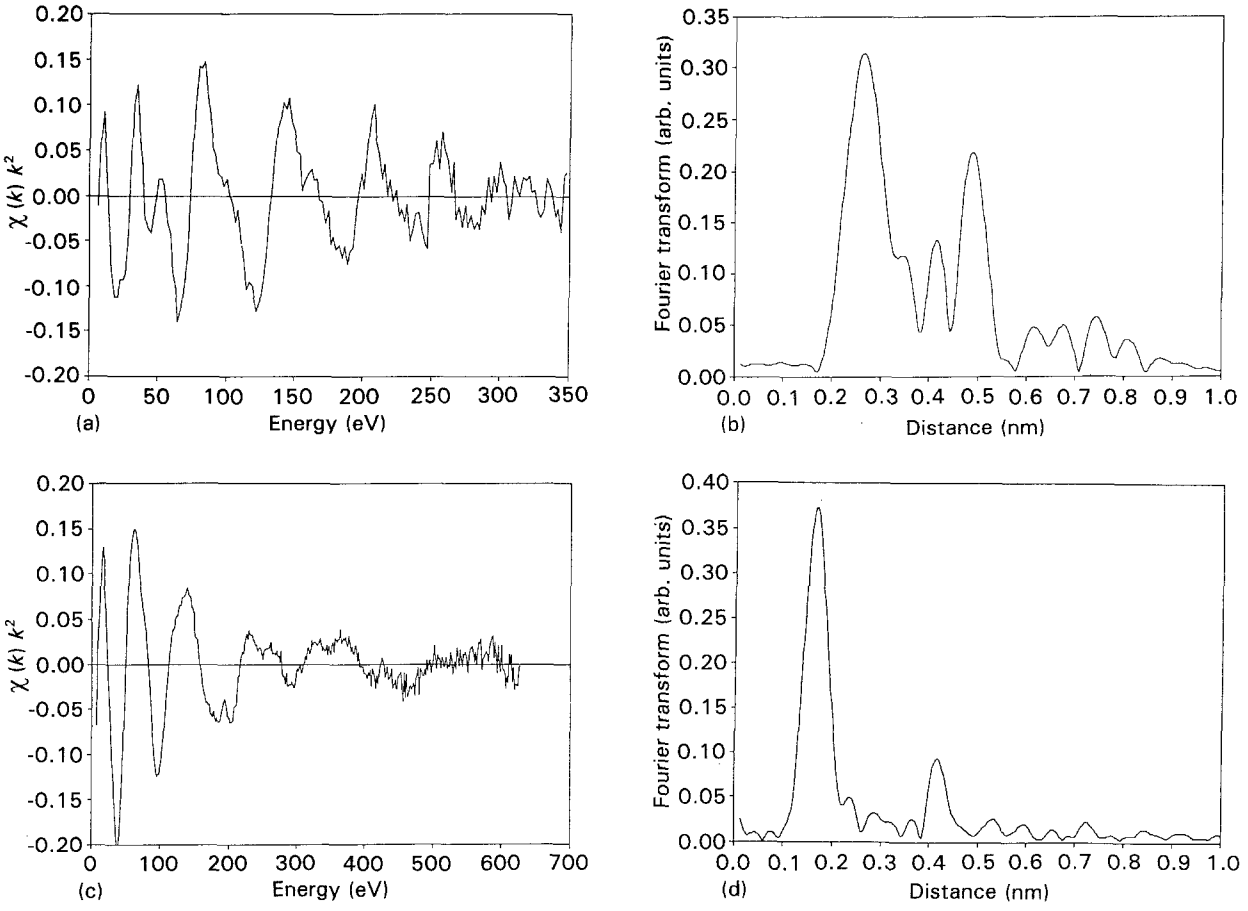

Figure 6 $RbBi_3F_{10}$: (a) Rb edge EXAFS; (b) Fourier transform; (c) Bi edge EXAFS; and (d) Fourier transform.

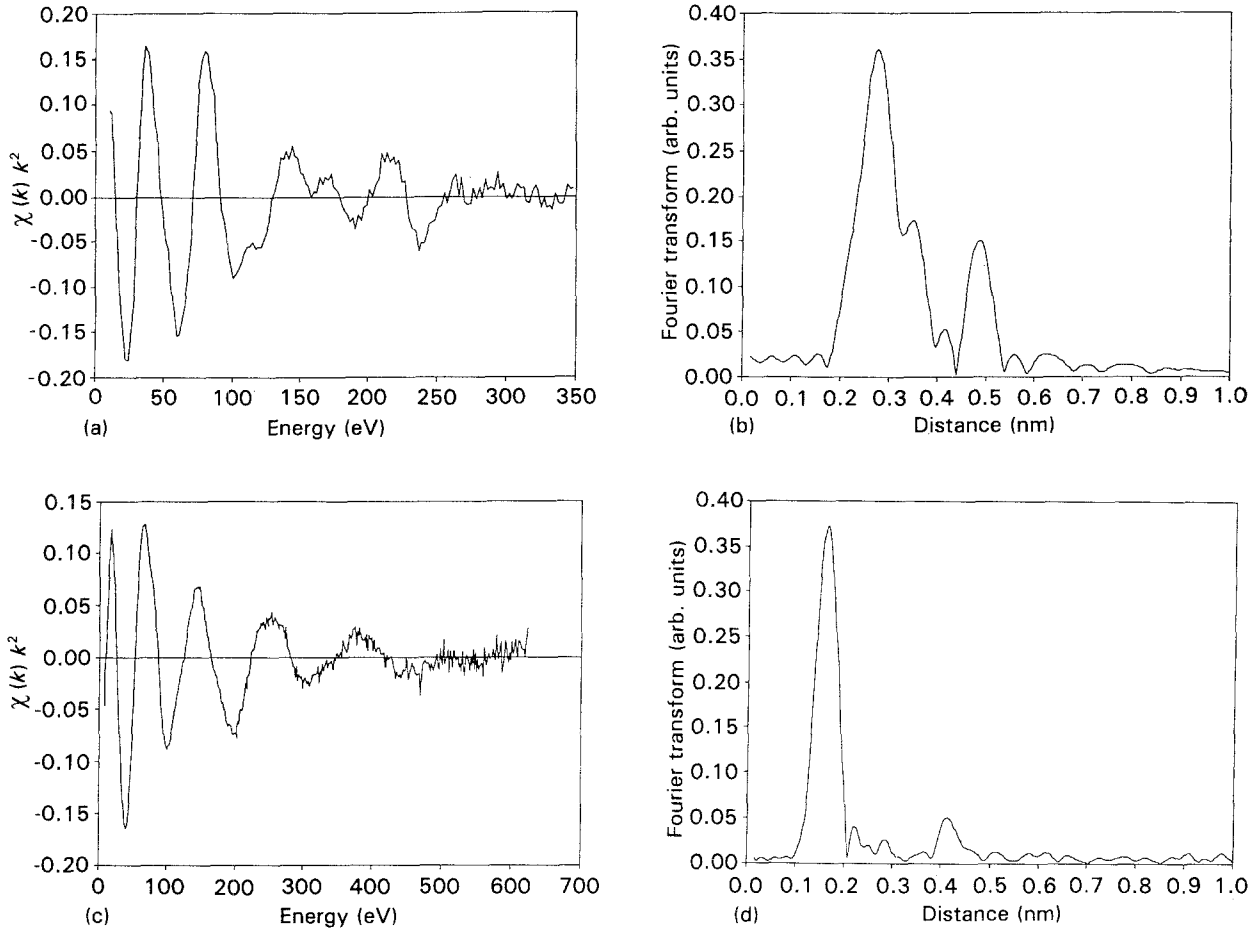

Figure 7 $Rb_{1-x}Bi_xF_{1+2x}$ ($x = 0.6$): (a) Rb edge EXAFS; (b) Fourier transform; (c) Bi edge EXAFS; and (d) Fourier transform.

shells must show a larger spread of component distances than in $RbBiF_4$.

2.3.3. $Rb_{1-x}Bi_xF_{1+2x}$ (x = 0.6)

The Rb and Bi edge EXAFS spectra for $Rb_{1-x}Bi_xF_{1+2x}$ ($x = 0.6$) at 80 K are given in Fig. 7. Inspection reveals

1. The degree of structure in the spectra is intermediate between that observed for $RbBiF_4$ and $RbBi_3F_{10}$. We can conclude that the degree of local ordering in $Rb_{1-x}Bi_xF_{1+2x}$ ($x = 0.6$) is between that of those two materials. This is confirmed by the two Fourier transforms which display fewer peaks than those obtained for $RbBi_3F_{10}$, but more than for $RbBiF_4$.
2. The peaks observed in the Fourier transform occur at the same positions as the ones in $RbBi_3F_{10}$. On this basis, we postulate that isolated cubo-octahedral clusters are present in the structure.

These results can be used to rationalize the trends in conductivity observed for $Rb_{1-x}Bi_xF_{1+2x}$ materials. As x deviates from 0.5, isolated cubo-octahedral clusters form, and a dramatic increase in local ordering is observed. Thus, increasing Bi content (and, therefore, adding additional charge-compensating F^- ions) does not increase the conductivity since F^- ions are trapped within these clusters, inhibiting diffusion. As x reaches 0.75, the clusters repeat in three dimensions to produce a fully ordered structure with a low conductivity.

3. Molecular dynamics

3.1. Computational details and results

3.1.1. $RbBiF_4$

Molecular dynamics simulations were performed on $RbBiF_4$ using the computer program FUNGUS [11] on the CRAY–XMP supercomputer at the University of London Computer Centre. Particles were initially assigned to the co-ordinates of the fluorite structure. Cations were randomly distributed over the available cation sites. A simulation box of 768 ions (256 cations and 512 anions) was used permitting a reasonable description of the random cation arrangement. The Buckingham interatomic potentials used in these calculations were derived from fits to the appropriate binary fluorides [12]. These parameters are given in Table I. As in previous MD simulations, polarizability were neglected, i.e. rigid-ion potentials were used.

TABLE I Buckingham parameters for interatomic potentials

	A (eV)	r (nm)	C (eV nm^6)
Rb–F	961.000	0.033 340	0.0
Bi–F	721.130	0.035 800	0.0
F–F	1127.700	0.027 530	2.68

Simulations were performed at three temperatures: 80, 473 and 750 K with a time step of 5×10^{-15} s. This is two orders of magnitude smaller than the minimum period of vibration in CaF_2 [13]. Each simulation was equilibrated until a constant temperature was obtained (at least 1000 time-steps) and then run for a further period of 3000 time-steps to yield a simulation time of 15 ps.

In Fig. 8 we present the calculated radial distribution functions (RDFs) for the two cations. These reproduce qualitatively all the features observed in the experimental EXAFS Fourier transforms (Fig. 5), specifically,

1. Both radial distribution functions contain only one well-defined peak, i.e. the high level of disorder in the material is modelled satisfactorily.

2. The peak in the Rb RDF is significantly broader and smaller than the Bi RDF, i.e. the static disorder in the Rb–F co-ordination shell is greater than in the Bi–F shell.

3. The peak in the Rb RDF is a distance of ~ 0.05 nm greater than the peak in the Bi RDF, i.e. the difference between the Rb–F and Bi–F bond lengths is accurately reproduced.

This agreement suggests that the equilibrium structure of the simulation is in excellent agreement with the actual structure. Analysis of the structure generated at 80 K shows that while the cations remain very close to their original input co-ordinates, the anions move to form a complex, grossly distorted "cubic" arrangement. The local environment of each cation is dependent upon the other cations in the co-ordination shell. A large number of fluorine ions are found to be close to the (0.33, 0.33, 0.50) interstitial site, especially near Bi^{3+} ions. The occupancy of the cube-centre site is also high (around 12% at 80 K). This contrasts strongly with other stoichiometric superionic fluorites, such as CaF_2, for which there is no evidence for high occupancy of the interstitial site in undoped materials. These results accord with the experimental results of Jordan [3] who postulated a two interstitial model for $RbBiF_4$ on the basis of fitting to neutron diffraction data.

Plots of the root mean square displacement $< R_\alpha^2(t) >$, of ion species α versus time for Rb, Bi and F are shown for the three temperatures in Fig. 9. At 473 and 750 K the upward gradient of the slope for $< R_F^2(t) >$ indicates that significant diffusion of fluorine ions is occurring. In contrast, no diffusion of cations takes place, even at 750 K, indicating that the simulated material is below its melting point.

The derived conductivities for the simulation are presented in Table II. The values obtained are lower than the experimental ones. Possible explanations for this are the omission of polarizability in the interatomic potentials and the fact that the program takes no account of lattice expansion as a function of temperature. As discussed by Catlow [14] polarizability

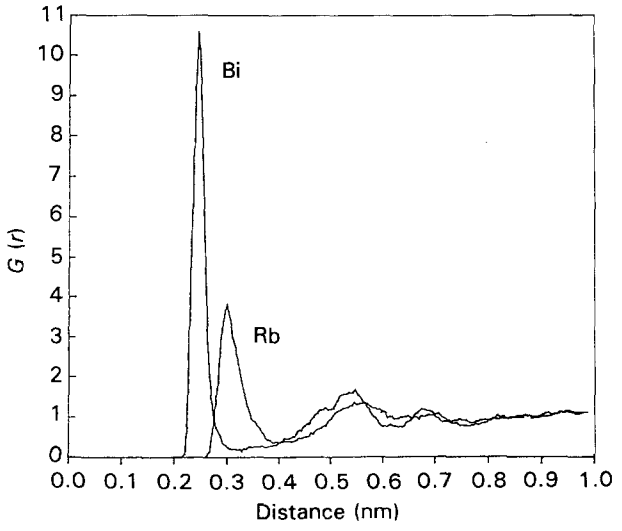

Figure 8 Calculated radial distribution functions [$G(r)$] for Rb and Bi at 80 K.

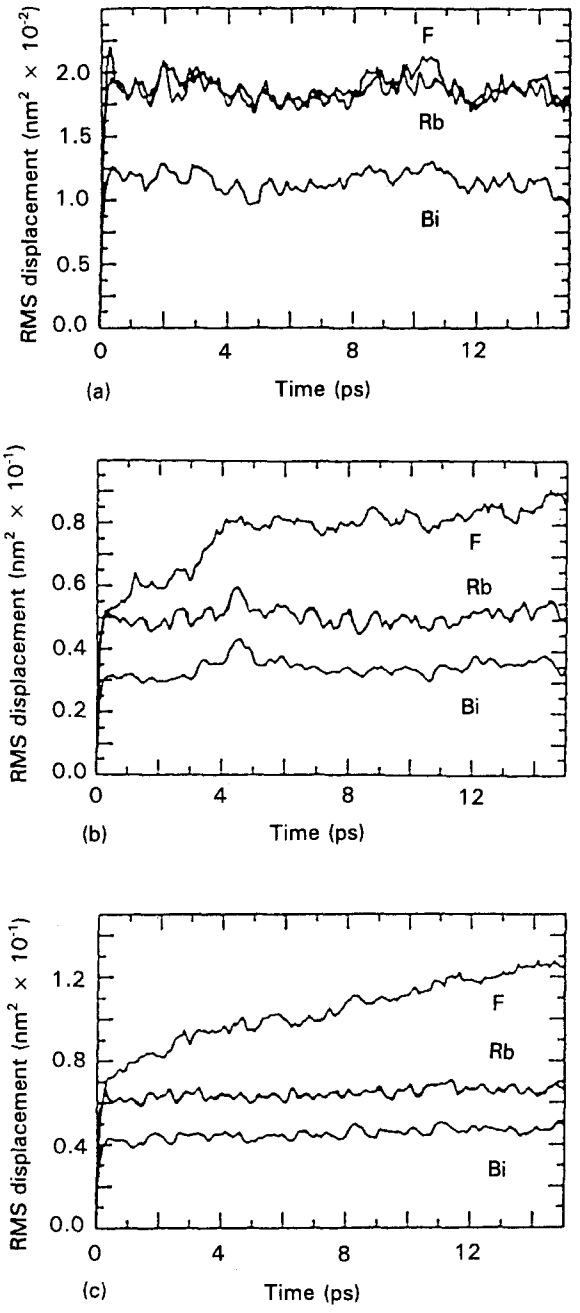

Figure 9 Root mean square (RMS) displacement versus time for Rb, Bi and F in $RbBiF_4$ at (a) 80 K; (b) 473 K and (c) 750 K.

TABLE II Transport coefficients for F^- ions in $RbBiF_4$

Temperature (K)	D_{calc} ($cm^2 s^{-1}$)	σ_{calc} ($\Omega^{-1} cm^{-1}$)	σ_{expt} ($cm^{-1} \Omega^{-1}$)
473	3.33×10^{-9}	2.53×10^{-3}	3.60×10^{-1}
750	5.56×10^{-7}	2.67×10^{-1}	1.40×10^{0}

can have an influence upon calculated properties. However, previous MD studies [15] have suggested that ion transport and structural information can be obtained, although quantitative values for diffusion coefficients and activation energies may be inaccurate.

Analysis of diffusing F^- ions at 750 K show that it is the cube-centre interstitials which play a key role in the diffusion mechanism. Fig. 10 shows a typical trajectory plot of a fluorine ion over 3 ps of the simulation. The ion is seen to move from interstitial site to an adjacent cube-centre site via a "perfect lattice" site by means of the non-collinear interstitialcy mechanism. Furthermore, the motion of migrating ions is co-operative as shown in Fig. 11, which displays the trajectories of three ions, one of which originally occupies an interstitial site. We note that the three ions move together, effecting exchange of F^- ions between lattice and interstitial positions. During the course of the simulation, even more complex concerted mechanisms are observed involving up to six F^- ions (Fig. 12). We postulate that this correlation of movement is almost certainly one of the factors promoting high F^- ion conductivity in these materials.

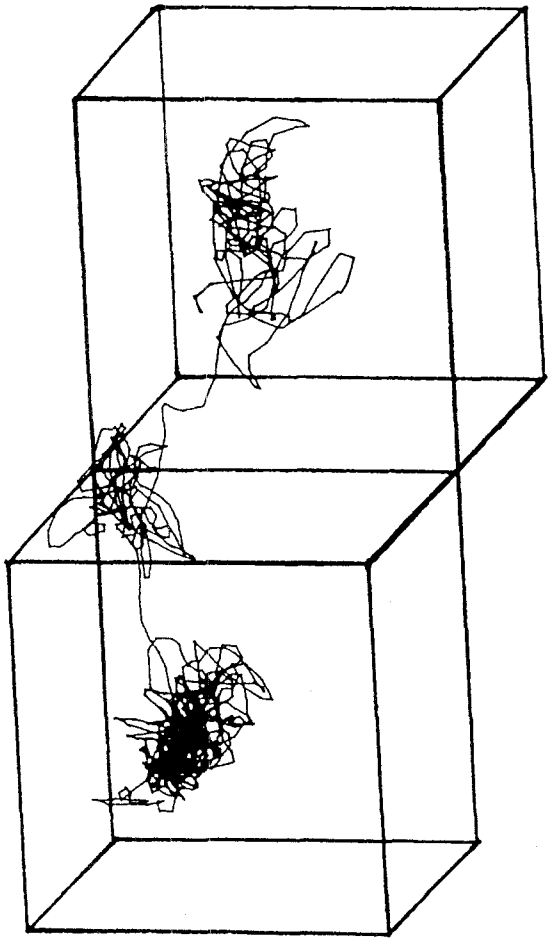

Figure 10 F^- ions migrate via a non-collinear interstitialcy mechanism.

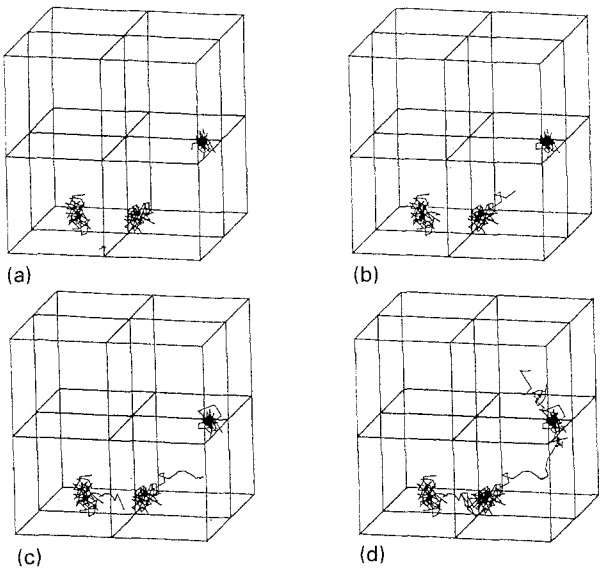

Figure 11 Four sequential 'snap shots' of three migrating ions.

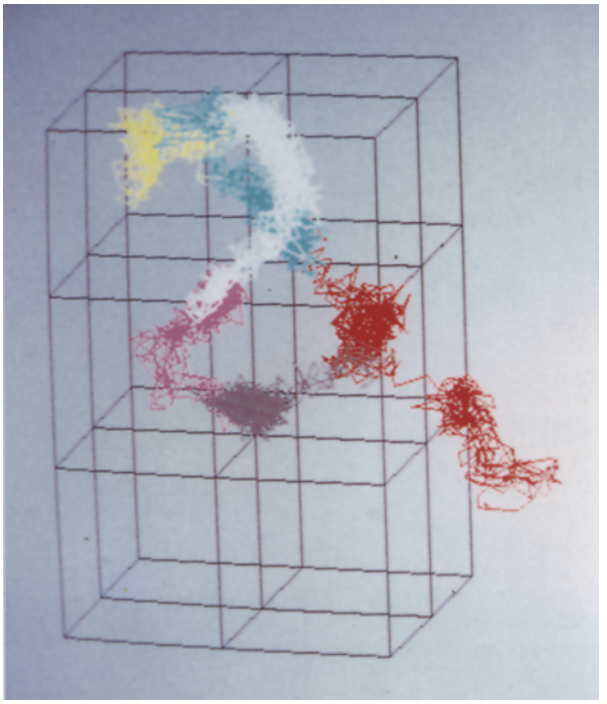

Figure 12 Six F^- ions migrating in a concerted mechanism.

3.1.2. $Rb_{1-x}Bi_xF_{1+2x}$ (x = 0.6)

Simulations were carried out on $Rb_{1-x}Bi_xF_{1+2x}$ ($x = 0.625$) at two temperatures, 80 and 750 K, the interatomic potentials were the same as those used for $RbBiF_4$. The simulation box contained 820 ions. Three different starting models were adopted,

1. The fluorite structure with cations randomly distributed over the available cation sites. Additional charge compensating fluorine ions were accommodated at cube-centre interstitial sites.

2. Structures based on the EXAFS data (a) The fluorite structure incorporating one $[RbBi_3F_8]^{2+}/[RbBi_3F_{12}]^{2-}$ cluster in the simulation box. Additional F^- ions not incorporated into these clusters were placed at cube-centre interstitial sites.
(b) As (a) above, but with two $[RbBi_3F_8]^{2+}/[RbBi_3F_{12}]^{2-}$ clusters per simulation box.

Plots of the root mean square displacement versus time for the three models at 750 K are presented in Fig. 13. For the model incorporating additional fluorine ions at interstitial sites with no cation ordering [model (1)] we observe an increase in the rate of fluorine ion diffusion over the $x = 0.5$ simulation. This disagrees with the experimentally observed result. Incorporation of clusters into the simulation box, however, reduces the rate of fluorine ion diffusion to below that of the $x = 0.5$ simulation. These results support the hypothesis from the EXAFS work that clusters form as x increases from 0.5.

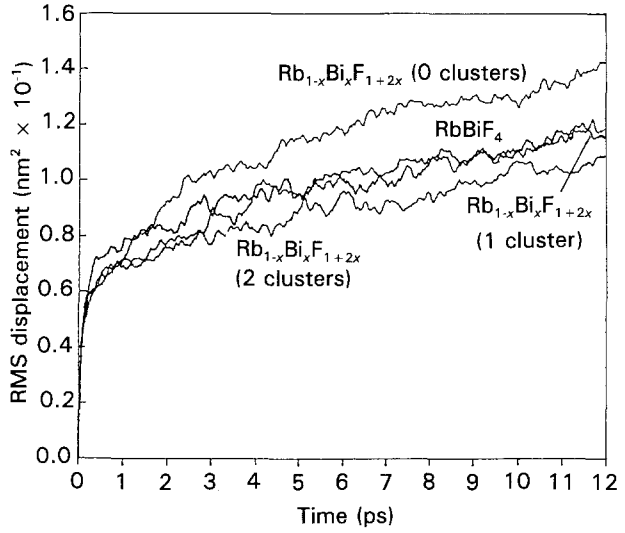

Figure 13 Root mean square (RMS) displacement versus time for F^- ions in $RbBiF_4$ and $Rb_{1-x}Bi_xF_{1+2x}$ ($x = 0.6$) with zero, one and two clusters per simulation box at 750 K.

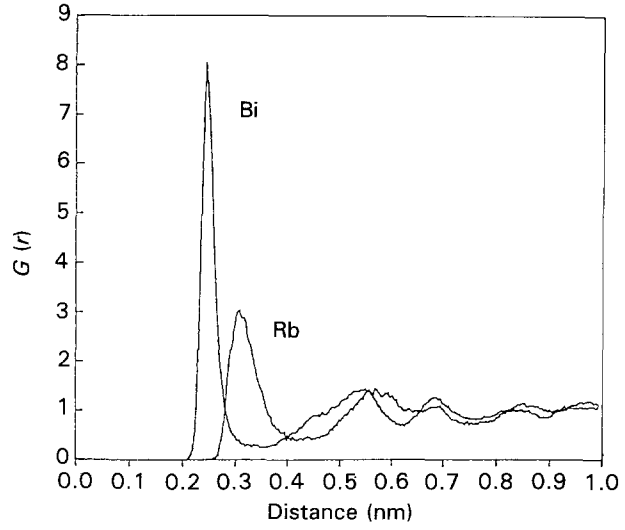

Figure 14 Radial distribution functions [$G(r)$] for Rb and Bi in $Rb_{1-x}Bi_xF_{1+2x}$ ($x = 0.6$) with two clusters per simulation box at 80 K.

It is also interesting to compare the RDFs for the $x = 0.625$ material with two clusters per simulation box (Fig. 14) with the RDFs obtained for the $x = 0.5$ material. We observe both a reduction in amplitude and broadening of the cation–anion nearest neighbour peak, in agreement with the changes observed experimentally. Motion of ions is via a non-collinear interstitialcy mechanism as for the $x = 0.5$ material.

We can conclude that as x deviates from 0.5, formation of cubo-octahedral clusters lowers the number of cube-centre interstitial sites available for migrating F^- ions which leads to a reduction in conductivity.

3.1.3. $RbBi_3F_{10}$

Molecular dynamics simulations were carried out on $RbBi_3F_{10}$ at two temperatures, 80 and 750 K. Interatomic potentials used were those given in Table I. Incorporated into the simulation box were 896 ions. Particles were initially assigned the coordinates of alternate $[RbBi_3F_8]^{2+}$ and $[RbBi_3F_{12}]^{2-}$ clusters, with a fully ordered cation sub-lattice.

In Fig. 15 we present the calculated RDFs for the two cations at 80 K. It can be seen that, in contrast to the simulations for $RbBiF_4$ and $Rb_{1-x}Bi_xF_{1+2x}$ ($x = 0.625$), a series of peaks is observed in the RDFs out to 1 nm, a feature indicative of long-range order in the simulated material. Examination of the equilibrated co-ordinates reveals that the input structure is extremely stable, with no deviation of ions from their

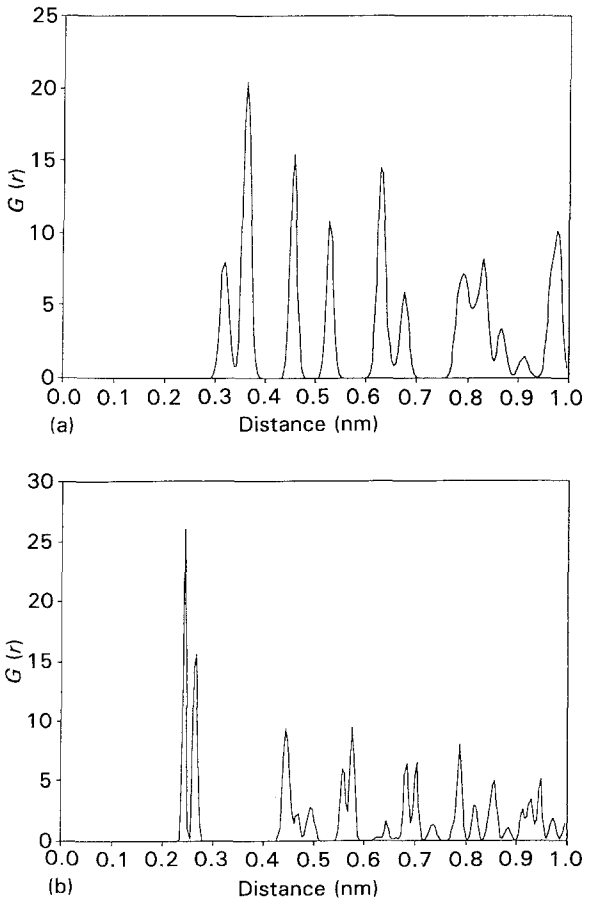

Figure 15 Radial distribution functions [$G(r)$] for (a) Rb, and (b) Bi in $RbBi_3F_{10}$ at 80 K.

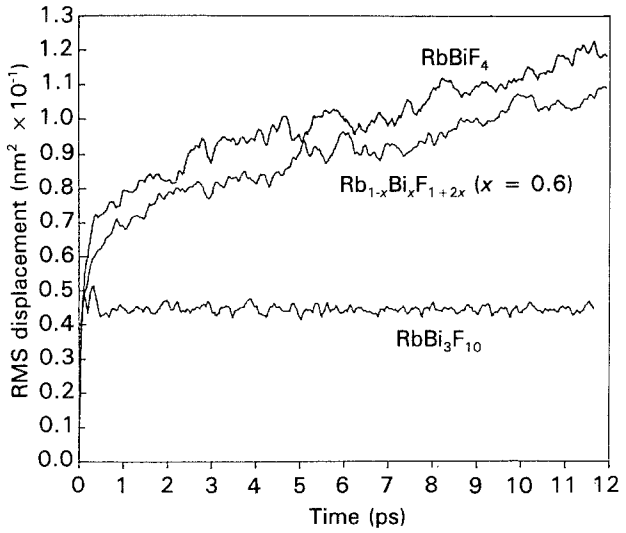

Figure 16 Root mean square (RMS) displacement versus time for F^- ions in $RbBiF_4$, $Rb_{1-x}Bi_xF_{1+2x}$ ($x = 0.6$) with two clusters per simulation box and $RbBi_3F_{10}$ at 750 K.

original co-ordinates. No diffusion of F^- ions is observed even at 750 K. Fig. 16 shows that the trends in diffusion rates for $RbBiF_4$, $Rb_{1-x}Bi_xF_{1+2x}$ ($x = 0.625$ with two clusters per simulation box) and $RbBi_3F_{10}$ accord with experimental measurements.

4. Conclusions

A random distribution of cations leads to uneven forces upon the F^- ions within $RbBiF_4$. This distorts the anion sub-lattice and forces many ions into interstitial sites, even at low temperatures. The cube-centre interstitials facilitate diffusion via a non-collinear interstitialcy mechanism, with correlation of motion helping to promote high conductivity. As x increases, cation ordering occurs which leads to the formation of cubo-octahedral clusters, as found in the $x = 0.75$ material. Within such clusters fluorine ions are trapped and hence the concentration of mobile cube-centre interstitials is reduced, thus diminishing the conductivity. On the basis of this work, an interesting experiment would be to attempt to synthesize $x > 0.5$ materials trying to prevent clusters from forming. One way of achieving this may be via rapid quenching techniques. Such materials we postulate would have higher conductivities than observed for $RbBiF_4$.

References

1. J. M. REAU, S. F. MATAR and J-L. SOUBEYROUX, *Solid State Ionics* **9&10** (1983) 563.
2. S. F. MATAR, PhD thesis, University of Bordeaux, Bordeaux (1983).
3. W. M. C. I. JORDAN, PhD thesis, University of London, London (1989).
4. J. W. PIERCE and Y. H-P. HONG, in "Proceedings of the 10th rare earth research conference carefree", edited by C. J. Kevane and T. Moeller, Vol. **A2** (NTIS, Springfield, Va, 1973) p. 527.
5. E. A. STERN in "Chem. anal". **92** (X-ray Absorpt.) (New York, 1988) p. 3.
6. P. A. LEE, P. H. CITRIN, P. EISENBERGER and B. M. KINCAID, *Rev. Mod. Phys.* **53** (1981) 769.
7. T. M. HAYES and J. B. BOYCE, *Solid State Physics* **37** (1984) 173.
8. M. J. GILLAN, *Physica* **131B** (1985) 157.
9. E. PANTOS and D. FIRTH, in "EXAFS and near edge structure", edited by A. Bianconi, L. Incoccia and S. Stipcich (Springer-Verlag, Berlin, 1983) p. 110.
10. C. R. A. CATLOW, A. V. CHADWICK, G. N. GREAVES and L. M. MORONEY, *Nature* **312** (1984) 601.
11. J. R. WALKER in "Computer simulation of solids", edited by C. R. A. Catlow and W. C. Mackrodt (Springer-Verlag, Berlin, 1982) p. 65.
12. C. R. A. CATLOW, M. J. NORGETT and T. A. ROSS, *J. Phys.* **C10** (1977) 1627.
13. M. J. GILLAN and M. DIXON, *ibid.* **C13** (1980) 1901.
14. C. R. A. CATLOW, *Solid State Ionics* **8** (1983) 89.
15. M. J. GILLAN, in "Solid state ionics '83", edited by H. Kloitz, B. Sapoval and D. Ravaire (Amsterdam, North Holland, 1983) p. 755.

Received 8 March
and accepted 31 August 1993